PRECISION DSN RADIOMETER SYSTEMS: Impact on Microwave Calibrations

C. T. Stelzried and M, J. Klein

Jet Propulsion Laboratory
California Institute of Technology
Pasadena CA 91109

Preprint of a paper to be published in

Design and Instrumentation of Antennas
for Deep Space Telecommunications and Radio Astronomy

Special issue of the IEEE Proceedings
February 1994
Guest Editiors: W. A. Imbriale and M. A. Thorburn

Printed (1 l/15193)

PRECISION DSN RADIOMETER SYSTEMS: Impact on Microwave Calibrations

C. T. Stelzried and M. J. Klein

Jet Propulsion Laboratory
California Institute of Technology
Pasadena CA 91109

ABSTRACT

The NASA Deep Space Network (DSN) has a long history of providing large parabolic dish antennas with precision surfaces, low-loss feeds and ultra-low noise amplifiers for deep space telecommunications. To realize the benefits of high sensitivity, it is important that receiving systems are accurately calibrated and monitored to maintain peak performance. A method is described to measure system performance and to calibrate the receiving system using procedures, software and commercial instruments that are easy to implement and efficient to use,

The utility of the measurement procedures and the precision of the receiver calibration technique were demonstrated by performing tests at K_a-band (32 and 33.68 GHz) frequencies at Goldstone on a 34-m beam-waveguide antenna Observations of multiple calibration radio sources are used to measure the dependence of antenna gain and system noise temperature on source elevation and derive the peak value.

Receiving system non-linearities are frequently overlooked as an error source in the calibration of microwave radiometers. The experimental results described in this paper illustrate some of the ways that receiving system non-linearity can negatively impact system performance. A simple radiometer calibration technique and analysis provide quantitative information that enables the system engineer to adjust and linearize the receiving system. When that is not practical, the experimenter or the operator can apply correction coefficients to the measured values of system noise temperature and thereby compensate for the receiving system non-linearity.

The high performance antennas and the sensitive receiving systems of the DSN are valuable resources for scientific research in addition to the primary telecommunication tasks that support space missions. The antenna gain and system noise temperature measurements and the radiometer calibration method described in this paper are also useful to perform precision research experiments.

1. INTRODUCTION

The NASA Deep Space Network (DSN) has a long history of providing sensitive receiving systems for deep space communications. These systems include large parabolic dish antennas with precision surfaces, low-loss feeds and ultra-low noise amplifiers. The sensitivity of these systems is characterized by measuring the receiving system figure of merit parameter G/Top (Ref 1,2) where G is the antenna gain and TOP is the system operating noise temperature (Ref 3). TOP includes contributions from cosmic noise, atmospheric emission, feed system

Printed (1 1/15/93)

losses and the receiving system thermal noise. The larger the G/T_{op} value, the more sensitive the system for spacecraft communications, radio and radar science and radio astronomy.

Over the past several decades the G/T_{op} parameter of microwave receiving systems has dramatically increased in the wake of technological developments and improved engineering practices. The G/Top for a microwave receiving system is optimized and calibrated and periodically monitored to detect potential degradation in performance. Potential sources of degradation include inclement local weather, physical antenna damage following severe rain and wind storms or, more rarely, earthquakes and routine modifications to the antenna feed and/or receiving subsystems,

Deep space planetary missions need reliable and current information of G/T_{op} to specify spacecraft telemetry data rates. The DSN, with 26, 34 and 70-m antennas, schedules the appropriate antenna size and performance to match the mission requirements. During critical mission phases such as planetary flybys, it is especially important to match antenna performance to the mission telecommunications requirements,

In this paper a set of routine procedures is developed to monitor the G/T_{op} parameter using radio sources and radiometers with high precision and minimal calibration time. Examples of performance measurements of the new NASA DSN Goldstone DSS 13 R and D 34-m beam-waveguide (BWG) antenna are presented and discussed. The data are analyzed to study the effects of receiver non-linearity on system performance, Considerable attention is given user friendly methods to verify and correct for receiving system non-linearity.

2. CALIBRATING LARGE MICROWAVE ANTENNAS

2.1 The G/T_{op} Parameter

The G/Top ratio is an accepted and useful parameter to quantify the sensitivity of microwave receiving systems that use large collecting areas and low noise microwave amplifiers (Ref 4). The gain of reflector microwave antennas is proportional to the collecting area of the surface divided by the square of the received wavelength (Ref 5). The system noise temperature is the result of several contributing sources. The G/T_{op} parameter is defined by

$$G/T_{op} = \frac{4 \pi A_e \lambda^{-2}}{T_a + \ldots} \qquad (1)$$

where A_e is the effective antenna area, λ is the received wavelength, TOP = (T_a + T_e) is the system operating noise temperature (Ref 3,4), T_a is the antenna noise temperature with contributions from the 2.73 K cosmic background, the earth's atmosphere (T_{atm}) and the antenna transmission line (T_t) and T_e is the effective

noise temperature of the receiving system with contributions from the low noise amplifier (T_{lna}), and the follow-up amplifier (T_f).

Precision measurements of the G/T_{op} of DSN antennas and their associated receiving subsystems are usually made when a new antenna is completed, when a significant upgrade is made to an existing antenna, and on a periodic basis for monitoring purposes. An effective method of obtaining G/T_{op} for microwave receiving systems is to measure the increase of the system noise when the antenna is pointed at a source of microwave emission with a known power density. In practice, the calibration source is usually selected from a list of astronomical radio sources whose microwave spectra have been accurately measured. The relationships between G/T_{op}, the power ratio measurement and the flux density of the calibration radio source are developed below.

The power ratio measurement is expressed as a Y-factor

$$Y = (To_p + T_s)/T_{op} \qquad (2)$$

where T_s is the increase in system noise temperature when the antenna is pointed at the radio source given by

$$T_s = S\, A_e/2k \qquad (3)$$

where S is the flux density of the radio source ($J\ m^{-2}$)*, k is the Boltzmann constant ($1.3807\ 10^{-23}\ J\ K^{-1}$) and

$$G = 4\ \pi\ A_e/\lambda^2 \qquad (4)$$

Substituting these equations into (1)

$$G/Top = (Y-1)\ (8\ \pi\ k/k1C_r\ \lambda^2\ S) \qquad (5)$$

where kl and C_r are constants accounting for transmission losses through the atmosphere and for the loss in received power for those cases where the angular dimensions of the radio source are partially resolved by the antenna beam, i.e., the angular dimensions of the calibration radio sources are small but they are not "point' sources. From equation (5) it is clear that G/Top can be calculated from the Y-factor measurement when the flux density, S, of the radio source is known. In practice, G/T_{op} for systems with large steerable antennas changes significantly as the pointing angle varies from horizon to zenith. The atmospheric component of system noise temperature increases with increasing zenith angle (decreasing elevation angle) while gravity distorts the structure as the antenna is tilted away (up or down) from the rigging angle (usually 45 degrees) where G is maximized by adjusting the surface panels. The dependence of G/Top on elevation angle is usually measured from a series of observations of one or more radio sources

* S is usually expressed in janskys where 1 Jy = $10^{-26}\ J\ m^{-2}$

over a wide range of elevation angles. The process usually requires more than 6 hours and often several days to complete.

The typical DSN antenna is instrumented with several receiving subsystems operating at different frequencies. Scheduling the time to calibrate G/Top for each DSN frequency band can be accommodated on an occasional basis, but routine monitoring is problematic. For the DSN, monitoring G/Top is simplified by measuring G and Top separately. G and its elevation dependence are assumed to be stable with time. T_{OP} is routinely monitored in the DSN as part of the spacecraft telecommunications procedures.

2.2 Calibration Radio Sources

The current method of calibrating operational DSN antennas using astronomical radio sources was standardized and documented after upgrading the 64-m subnet to 70-m diameter antennas (Ref 6). The use of radio sources for this purpose has been in use for decades by the radio astronomy community and has been adopted by the DSN. This method measures the antenna gain by using the broad band flux densities of a selected set (Ref 7,8,9,1 O) of galactic and extra galactic radio sources sufficiently well-known to be used as calibration standards. The advantage of this approach is that these astronomical radio sources, which are distributed over the entire sky, can be measured day or night at virtually any position in the sky. The method has been used very successfully to measure the relative changes in antenna gain vs elevation angle as the radio sources rise and set.

A difficulty of this approach involves the accuracy of the measurements, which depends upon knowledge of the radio flux densities, the angular size of the emission region, and the intensity variations with time. Fortunately, enough is known about the list of calibration sources so that measurements of relative changes can be made with 2-sigma precision of approximately 0.15 dB and measurements of absolute gain can be made with a 2-sigma accuracy of approximately 0.5 dB.

Source lists for calibration at frequencies above 20 GHz often include the brighter planets such as Venus and Jupiter. In contrast with most astrophysical radio sources, the flux density of a planet increases rather than decreases with increasing frequency and for this reason planets tend to be the strongest continuum radio sources at wavelengths shorter than about 1-cm. Furthermore, the flux densities from planetary atmospheres and/or surfaces can be calculated from detailed thermophysical models developed from data returned by numerous spacecraft that have been sent from Earth.

3. A PRACTICAL METHOD TO DETERMINE G/T

3.1 Receiving System Calibration Instrumentation

The operational Deep Space Network (DSN) uses noise adding radiometers (NARs) 10 perform antenna gain and noise temperature calibrations for telecommunications performance analyses (Ref 6). The NAR configuration, developed in the 1970s, uses a microwave noise diode as a reference to compensate for gain fluctuations in the maser low noise amplifier (LNA). The performance of the NAR configuration is significantly better than the total power radiometer (TPR) configurations that it replaced. It has been successfully used in the DSN for almost two decades.

As part of an effort to provide DSN operators with efficient and convenient methods to maintain accurate calibrations of microwave radiometers, a modest research and development activity was carried out at the Goldstone DSS 13 Venus R and D station. The objective was to develop user friendly methods to measure system noise temperature and antenna gain with improved accuracy and to replace special purpose detectors and computers with commercially available equipment.

The development work began with a NAR configuration similar to those used in the operational DSN. A TPR, which uses a commercial digital power meter detector, was also assembled and tested because it had the potential of being a more reliable and cost-effective configuration. TPRs are now competitive with gain stabilized systems, such as the NAR, because of recent advances in low noise amplifiers and follow-on receiver hardware as well as improvements in modern computer technology that accommodate frequent radiometer calibrations as part of the observation data strategy.

Figure 1 near here

Figure 1 represents the TPR configuration that was used to develop and test calibration techniques at the Venus Station on the 26-meter antenna at S- and X-band (2.3 GHz and 8.4 GHz) and recently on the new 34-m beam-waveguide (BWG) antenna at X-band (8.4 GHz) and K_a-band (32 GHz and 33.68 GHz); see references 11, 12, 13 and 14. The radiometer system includes the antenna feed, an ambient temperature load, a microwave switch, a calibration noise diode, a readout device and receiving system. The readout device for the TPR is a Hewlett Packard 438-A digital power meter. The receiving system usually consists of a LNA, mixer and IF amplifiers. The signal level is adjusted to provide an output of about 2 uwatts when the microwave LNA input is connected to the ambient load.

The ambient load has traditionally been a waveguide termination that is accessed through the waveguide switch. This configuration was modified to take advantage of the benign environment of the instrumentation room located in the basement of the BWG antenna. The waveguide switch was removed and the waveguide load was replaced with an aperture load attached to a movable arm designed 10 swing the load in a plane located above and perpendicular to the feed aperture. The insertion loss of the microwave feed assembly is reduced with the removal of the waveguide switch.

The gain of the TPR receiving system will usually drift with time and/or changes in ambient temperature, Experience has shown that modern LNAs, follow-on amplifiers and commercial power meter detectors are stable for short-term variations (1 minute). However, it is very important to account for long term drifts in the end-to-end gain of the TPF? receiving system. Extensive tests of a variety of TPR receiving systems used at Goldstone over the past 5 years have demonstrated that gain drifts are relatively small (< 5% over several hours) and sufficiently slow that gain variations can be accurately tracked if calibrations are made two or three times per hour. These "observing calibrations" or "minicals" require less than 1 minute to complete, so they are only minor interruptions to the observational sequence. An example of a typical calibration sequence is discussed in Section 4.1.

The method applies equally well to a NAR with a square law detector or to a Dicke switching system with a phase sensitive detector. For the NAR system, a second noise diode is needed to provide the noise modulation at the LNA input.

3.2 The radiometer calibration method

The radiometer calibration data are recorded from the readout device as the system is configured to five different states. The readout, R1, of the first state is the bias with the readout device input terminated in a matched load. Ideally R1 should be exactly zero, but in some configurations it has a small but non-zero value. The second and third states are recorded with the LNA input connected to the antenna and the antenna is directed at the cold sky with the noise diode off (R2) and diode on (R3). The LNA input is then connected to the ambient load for the fourth and fifth states where R4 is recorded with the diode off and R5 is recorded with the diode on. The readout device bias R1 is subtracted from each of the other four readouts before subsequent computations are made. Figure 2 is a schematic showing the relationship between system readout (with bias reading removed) and input noise temperatures for a linear system and a hypothetical system with severe" non-linearity.

Figure 2 near here

When the ambient termination is properly matched, the system noise temperature with the receiving system input connected to the ambient load is given by

$$T4 = T_p + T_e \qquad (6)$$

where T_p is the physical temperature of the termination (load) which is typically measured with a digital thermometer, and l-e is the receiving system noise temperature, which is assumed known from separate calibrations, In low noise systems T_e is small compared to T_p so that a small percentage error in T_e contributes a smaller percentage error in T4 (Ref 15). For example, if T_p = 290 K and T_e = 10 K, a 10 percent error in T_e results in only a 0.33 percent error in T4.

The radiometer receiving system gain is defined by the ratio

$$B = T4/R4 \quad (7)$$

Assuming the system is linear, the system noise temperature with the LNA input connected to the antenna is given by

$$T2 = B\ R2 \quad (8)$$

where T2 = Top with the antenna pointing at a "cold sky" calibration position, which in many cases is near the zenith. If a radiometer receiving system is not linear, the relation between T and R will deviate from the simple proportion of equation (8) as discussed in Appendix A. To compensate for the deviation, the corrected system noise temperature on the antenna is defined by

$$T2C = BC\ T2 + CC\ T2^2 \quad (9)$$

The constants BC and CC are calibrated using the noise diode associated with readings R3 and R5 described above. The linearity of the receiving system is evaluated by comparing the two readout Increments (R5-R4) and (R3-R2). For a perfectly linear system, these two increments will be equal and the two constants will be BC =1 and CC = O. A quantitative indication of a non-linear system is given by the magnitude of the difference between T2C and T2. Details of the method and the analysis are given in appendix A.

Tests made with non-linear systems suggest that equation (9) can be used to reduce measurement errors whenever stable, calibrated values for the constants BC and CC are known:

$$Top(corrected) = T_{OP}C = BC\ TOP + CC\ T_{op}^2 \quad (Io)$$

However, the best practice is to identify the receiver non-linear elements and then adjust the system operating conditions for linear performance (see section 3.3).

3.3 The Issue of Radiometer Dynamic Range

The radiometer receiving system non-linear performance has proven to be a troublesome component of the error budget for the measurement of DSN antenna parameters. An example of the problem surfaced when it was discovered that system temperature measurements taken with the NAR did not agree with those taken with the TPR. The problem persisted even when the NAR algorithms were adjusted to compensate for non-linearity in the square law detector (use of an "alpha" coefficient, described in Ref 16). Further analysis indicated that radiometer receiving system non-linearity might explain the conflicting results and the test procedure was modified to measure the end-to-end linearity of each radiometer receiving system configuration.

The utility of the test procedure was demonstrated at Goldstone in November 1992 when a K_a-band receiving system was installed on the 34-m BWG antenna at DSS 13. A TPR system was implemented with a 32 GHz maser low noise amplifier in the BWG pedestal room and the calibration tests described in this paper were carried out. The data corresponding to the five measurement states are shown graphically in Figure 3. The results, which gave system temperatures of T2 = 50.6 K and T2C = 45.7 K, indicated that the receiving system non-linearity (obtained from T2/T2C) was approximately 110/0 as measured on 11/1 0/92. Attenuator pads were inserted at the inputs to key elements in the receiver amplifier chain to optimize the gain profile and linearity of the system. When the calibration procedure was repeated (1 1/18/92), the measured system temperatures of T2 = 46.0 K and T2C = 45.6 K indicated non-linearity less than 1%. It is interesting to note that the values of T2C before and after reducing the receiving system non-linearity agreed within 0.1 K (also less than 1%) providing confidence in this calibration method. These results demonstrate that the optimization and calibration sequence is effective.

Figure 3 near here

The non-linearity of the receiving system shown in Figure 3 might not appear to be severe at first glance. However, an 11 % non-linearity produces significant degradations to the error budget of system performance measurements. Moreover, these effects tend to be systematic rather than random, so they are often overbooked.

An example of the insidious impact of receiving system non-linearity is illustrated in Figure 4 **where the values of T2 (linear analysis) and T2C (non-linear analysis)** are plotted for three different radiometer test configurations on the 26-m antenna at 0SS 1:3 in 1987. The objective was to compare the calibration results of a NAR and two TPR systems using the linear and the non-linear analysis methods (Ref 17). The NAR and one of the TPR systems used a detector that was known to be several percent non-linear. The TPR with a power meter detector was expected to be the most linear anti the most accurate of the three configurations.

Figure 4 near here

The results of the three calibrations with linear analysis gave T2 values (solid dots) that fell in the range of 30.8 to 31.9 K. In contrast, the non-linear analysis produced results that converged to T2C = 31.85 +/- 0.05 K (open circles). This average value of T2C was very close to the value of T2 for the TPR configuration that was believed to be the most linear at the outset,

Receiving system linearity is important to verify and easy to overlook when new systems are installed or when existing systems are modified. The calibration method described in this section is an efficient technique to evaluate and monitor end-to-end receiving system linearity,

4. **TESTING,** VERIFYING AND APPLICATION

4.1 Test Observations

The DSS 13 Venus station provides a facility to test instrumentation and verify the analysis used to measure system noise temperature and antenna efficiency. In March 1993a K_a-band HEMT low noise amplifier was installed at one of the receiving! system stations in the pedestal room of the BWG 34-m antenna. The TPR system described in Section 3.1 was implemented to test the system at 33.68 GHz. The detector is a Hewlett Packard 438-A digital power meter which is specified to provide linearity better than 99%. Evaluating the receiving system linearity was one of the test objectives of the calibration measurements.

The radio sources selected for the calibration tests were Venus, Jupiter and the radio Galaxy Virgo A, which is one of the better understood radio sources used for antenna gain measurements. Venus and Jupiter are "bright" K_a-band. radio sources where flux densities can be calculated with estimated 2 sigma accuracy of +/- 8% (absolute flux scale). Furthermore, these particular sources were selected because their flux densities differed by a wide margin from the weakest (Virgo A @ 14 Jy) to the strongest (Venus@ 1060 Jy). This range of source intensities proved to be useful for the receiving system linearity tests described in Section 4.3.

The 1993 observations were made between O and 08 hours UT on April 1 (DOY 091) and between 22 hours UT April 7 and 09 hours UT on April 8 (DOY 098). The radio source noise temperatures were measured using an orthogonal 5-point antenna pointing sequence. The TPR measures and records Top while the antenna beam pointing offset is zero in one coordinate and the beam position is stepped through 5 offset positions ($x_1 \ldots x_5$) in the orthogonal coordinate. The offset values are $x_i = n_i$ x HPBW, where n_i = +5, +0.5, O, -0.5, -5 and HPBW = one half-power beam-width (the full width between +/- 3 dB points). The ten values of Top are then processed to evaluate the peak source temperature and adjust for residual pointing offset errors, which were typically less than +/- 0.1 HPBW.

Precision calibration sequences of the radiometer were conducted before (PRECAL) and after (POSTCAL) the observing sessions on the two dates. The data for each PRECAL and POSTCAL consists of a set of six measurements of R1 through R5 described in section 3.2. The results are average values and standard deviations of the TPR receiver gain and system linearity coefficients (B, BC, and CC).

Figure 5 near here

The TPR receiving system gain calibration was re-measured periodically at least twice each hour through the observing session. The results of these "observing calibrations" (OBSCAL) were used to update the TPR receiving system gain coefficients and thereby compensate for slow variations of gain. The April 1 OBSCAL receiving system gain data, expressed as ratios relative to the precal gain, are shown in Figure 5. The trend and the scatter of the data are representative of calibration data taken on many occasions, Experience has

shown that errors in the updated TPR receiving system gain are usually less than 0.5% when this procedure is followed.

The PRECAL and POSTCAL data were combined to evaluate the TPR system linearity for the two dates. The results show that the receiving system non-linearity was <1% during these observations: T2/T2C = 0.992 on April 1 and 0.994 on April 7/8. The PRECAL results were within +/- 0.001 of the POSTCAL results on both days.

4.2 Aperture Efficiency Results

The radio sources were observed over a wide range of elevation angles to calibrate the changes of aperture efficiency as the antenna pointing angles vary from horizon to zenith. The aperture efficiency, η, is the ratio of the effective aperture A_e and the geometric aperture A_g of the paraboloid.

$$\eta = A_e/A_g = 4\ A_e / \pi\ D^2 \qquad (11)$$

where D is the aperture diameter. Substituting equation 3 (section 2.1), equation 11 can be rewritten

$$\eta = 8\ k\ T_s^* / \pi\ D^2\ S \qquad (12)$$

where

$$T_s^* = C_r\ T_s \qquad (13)$$

and C_r > or = 1 is a correction factor applied to the observed source antenna temperature, T_s, to adjust for the loss in signal that occurs when the antenna beam partially resolves the solid angle of the source, which is either a circular or elliptical disk when the source is a planet.

Individual values of η for each measurement of T_s can be calculated for known values of flux density (S) and C_r that are listed in Table 1. The value of C_r = 1.28 +/- 0.02 for Virgo A was measured in August 1993 by comparing two-dimensional brightness temperature maps of Virgo A and the quasar radio source 3C 273, which is sufficiently compact to serve as a "point source" calibrator for the 34-m antenna at K_a- band frequencies.

Table 1: Source Flux Densities and Peak Temperatures

Common Name	IAU Designation	S(33.68GHz) Jy	Ref	Cr	T(Source) (eff=100%)
Venus (Apr 1)	---	1051.8	18	.342	257.6
Venus (Apr 8)	---	1004.1	18	.326	249.1
Jupiter (Apr 1)	---	164.3	19,20	.168	46.25
Jupiter (Apr 8)	---	163.6	19,20	.167	46.10
rgo A (3C 274)	1228 + 126	14.1	6	1.28	3.608

Note 1: Planet fluxes were calculated from referenced disk brightness temperatures [Venus Tb = 460 K; Jupiter Tb = 140 K] with compensation for the planet's distance from Earth.
Note 2: IAU = International Astronomical Union

Combining equations 11 and 12, and setting $\eta = 1$ gives an expression for source temperature for a "perfect" antenna:

$$T_S(100\%) = \pi D^2 S/8 k C_r = 2,8442X10^{-22} D^2 S/C_r \quad (14)$$

A useful alternative expression for the aperture efficiency is

$$\eta = T_S/T_S(100\%) \quad (15)$$

Values of $T_S(100\%)$ are shown in the last column of Table 1.

The aperture efficiency measurement data are plotted as a function of elevation angle in Figure 6. Each value of T_S was adjusted to compensate for the attenuation by the terrestrial atmosphere. The attenuation is compensated from ground weather parameters assuming a horizontally stratified flat-earth model for the troposphere and a simple (l/sin) dependence on elevation angle (Ref 21). The efficiency peak of 0.43 near elevation angle 55 degrees matches the curves from the more extensive measurements reported in Ref. 22 and summarized in Ref. 1.

Figure 6 near here

The data associated with the three calibration sources, identified by different symbols in Figure 6, are consistent. The agreement can be quantified by separating the data into three sets and independently solving for the peak aperture efficiency. The results from the calibration observations taken at 33.68 GHz are listed in column 3 of Table 2. The corresponding values of the peak

antenna gain at are listed in the fourth column. The average value of the peak gain is 7'7.94 dB and the corresponding G/T_{op} is 59.08 dB, where Top= 77 K is the average system temperature that was observed near 55 degrees elevation.

Table 2: Calibration Results at 33.68 GHz for 34-m Beam Waveguide Antenna at DSS 13 (Goldstone)

Source Name	Peak Ts K	Peak Efficiency	Peak Gain dB
Venus	110	0,431	77.92
Jupiter	19.9	0.432	77.93
Virgo A	1,57	0.436	77.97
Averages:		--0.433	77.94

The peak efficiencies for the three sources differ from the average value by less than 0.005 . This result suggests that the microwave spectra of the two planets at short centimeter wavelengths have been accurately calibrated and that the measured value of C_r for Virgo A leads to a consistent result for that source as well. Absolute calibration measurements of the Ka-band spectra of these three sources are the subjects of a current study by the authors of Ref 23.

For the present 0SS 13 34-m antenna HEMT LNA configuration, Top = 77 K at 55 degrees elevation. This results in a peak estimate of G/T_{op} = 59.08 dB for K_a-band near 55 degrees elevation angle, but G/Top actually peaks at a slightly higher elevation angle because the system noise temperature varies from a maximum at low antenna elevation angles to a minimum at zenith.

4,3 Receiving System Non-linearity Effects

The agreement in the data in Figure 6 and Table 2 would not have been so close had a non-linear receiving system been used for the observations because the errors introduced by radiometer non-linear performance are not uniform with source temperature magnitude. To demonstrate this dependence, the data taken in November 1992 with the non-linear receiving system described in Section 3.3 were subjected to the linear and the non-linear analyses.

The percentage error caused by the non-linearity, given by equation Al 4 in the appendix, is a function of the calibration temperatures T4, T_{off}, (system noise temperature with antenna off pointed in the region of a nearby radio source calibrator), T_s (the radio source noise temperature contribution), and the linearity coefficient CC. For the 11/1 0/92 data, T4 = 340.1 K and CC = 3.33394 x 10^{-4} and T_{off} = 50.6 K. Using these parameters, the percentage error in measurements of T_s were calculated for hypothetical values of T_s in the range 10 K to 200 K. The results are shown in the appendix (Figure Al) and summarized here in Table 3 for three values of the system temperatures near zenith that are representative of a HEMT (T_{off} = 70 K), the maser/dichroic configuration of November 1992 (T_{off} = 50 K) and the maser/dichroic configuration (T_{off} = 30 K) that is expected to be realized in the future at 0SS 13 (Ref 24).

Table 3: Example of Errors Caused by 11 % Non-linearity in an **Unoptimized** TPR System

Hypothetical Source Temperatures, T_s			
T_s, K	T_{off} = 30 K	T_{off} = 50 K	T_{off} = 70 K
	T_s Measurement Errors, %		
10.	9.9	8.3	6.8
100.	6.4	4.9	3.5
200.	2.7	1.4	0.0

Sources Observed in April 1993

Sources	T_{off} = 30 K	T_{off} = 50 K	T_{off} = 70 K
	Hypothetical Antenna Gain Measurement Errors, dB		
Venus	0,27	0.21	0.14
Jupiter	0.41	0.34	0.28
Virgo A	0.45	0.38	0.31

Table 3a. DSS 13 34-m antenna radio source T_s calibration non-linearity measurement errors with unoptimized radiometer system based on 11/10/92 evaluation (Upper Frame).
Table 3b. Effect that 11 % radiometer non-linearity would have had on antenna gain calibration measurements of April 1993 (Lower Frame).

An example of the impact of radiometer receiving system non-linearity on antenna gain measurements is shown in the lower panel of Table 3. Had the gain measurements of April 1993 been made with a 11 **%** radiometer **non-linearity, the results for the three sources would have been in error by the** amounts listed in the last column of the table (T_{off} = **70** K). The hypothetical TPR non-linearity would have caused the antenna gain results from the three sources to diverge as the non-linearity caused antenna measurement error increased from 0.14 dB for Venus to 0.31 dB for Virgo A. The average value of the gain would have been incorrect and the scatter of the three data values would have been 2.8 times greater than the variance of the experimental data.

TPR receiving system non-linearity errors are increased as the system noise temperature decreases and are minimized for source temperatures T_s = T4 -2 T_{off}

4.4 Receiving System Non-linearity Effects and Variable Radio Sources

Measurements of radio source **flux densities with non-linear TPR receiving** systems may produce pathological results that are exacerbated if the radio source intensity is time variable. Many galactic and extragalactic radio sources are known to exhibit intensity variations, and measurements of these sources will be biased by the non-linear errors that arise as T_s changes, The effect is small (<0. 1 dB) for most sources because the amplitude of the intensity variations is usually much less than fifty percent.

Printed (1 1/1 5/93)

Receiving system non-linearities produce errors that maybe surprisingly large when the brighter planets are observed at short centimeter or millimeter wavelengths. A prime example of the problem can be derived from the 1993 Venus measurement at 33.68 GHz. The observations were made when Venus was near inferior conjunction, i.e., the time when the distance between Venus and the Earth is a minimum. The flux density of Venus was close to its maximum value early in April, but it was decreasing each day as the planet's orbital motion carried it farther from Earth. In fact, the intensity of Venus vanes by a factor of *thirty eight* as the planet's distance varies from 0.28 to 1.72 astronomical units.

Figure 7 shows the predicted error that would result if measurements of Venus were used to calibrate G/Top for the 34-m BWG antenna at 33.68 GHz using a TPR receiving system that is 11% non-linear. The plot shows the absolute error that would be expected as a function of the planet's 19-month synodic period , P_S and the time of the observations, t (months). Note that the error is a minimum (0.1 4 dB) near x = t/P_S = 0.5, when Venus is closest to Earth and that it increases to 0.27 dB as Venus reaches maximum distance at x = 1 (Superior Conjunction). If measurements were spread over this time span, G/T_{op} would appear to vary as much as 0.13 dB.

Figure 7 near here

As an example of the effect of non-linear receiving system errors, consider a hypothetical experiment whereby a non-linear TPR is used to measure the brightness temperature of Venus. If the experimenter were unaware of the non-linearity, the variations in systematic error shown in Figure 7 might be mistakenly attributed to changes in the brightness temperature of the planet. In fact, the variation might readily be accepted as evidence of a phase angle dependence because the error induced variability is so tightly coupled with the orbital period.

5. CONCLUSIONS:

The sensitivity of DSN receiving systems has dramatically increased as a result of three decades of technological advances and improved engineering practices. To realize the benefits of high sensitivity, it is important that receiving systems are accurately calibrated and that G/Top measurements are repeated over time to maintain peak performance. The method described in this paper is designed to measure system performance in terms of G/T_{op} and includes a technique to calibrate the radiometer system using procedures, software and commercial instruments that are easy to implement and efficient to use. The radiometer calibration only requires a few minutes to complete and the G/Top measurements are typically accomplished in about 10 hours.

The utility of the calibration technique and the measurement procedure was demonstrated by performing tests on receiving systems operating at K_a-band frequencies on the 34-m BWG antenna at DSS 13. One of the tests consisted of observing calibration radio sources over a wide range of elevation angles. The observations were made by interleaving system radiometer calibrations with radio source intensity measurements, which were accomplished using an automatic boresight technique. Three calibration radio sources were selected to validate the

use of multiple sources to measure the dependence of G/Top on radio source elevation angle. The advantage of multiple radio sources is the ability to measure G/T$_p$ at many azimuth and elevation angles in a single observing session of 8-12 hours.

A plot of the observational data produced a smooth curve of antenna aperture efficiency vs elevation angle that peaked at 43% near 55 degrees. The corresponding peak antenna gain is G = 77.94 dB at 33.86 GHz. The results from the three different radio sources are mutually consistent even though their relative intensities ranged from 1.5 K to 105 K.

An important component of the TF'R system calibration method concerns the receiving system linearity, which is measured and quantified with sufficient accuracy that the impact on system performance can be assessed. The analysis of the experimental data showed that G/Top can be measured with a two-sigma precision of the order +/-0.15 dB if the receiving system is linear. The analysis also indicated that even modest (<10%) TPR non-linearity can affect the absolute measurement accuracy as much as +/-0.5 dB and can lead to discrepancies in the measurement of system temperature (To_P) and G/T_{op}.

Receiving non-linearities are frequently overlooked as an error source in the calibration of microwave radiometers and antenna measurements. The experimental results described in this paper illustrate some of the ways that radiometer non-linearity can negatively impact system performance. The calibration techniques and analysis provide quantitative information that enables the system engineer to adjust and linearize the receiver. When that is not practical, the experimenter or the operator can apply correction coefficients to the measured values of Top and thereby compensate for the radiometer non-linearity.

7. REFERENCES

1. W. Rafferty, et al, “Ground Antennas in NASA’s Deep Space Telecommunications: Past Present and the Future,” this issue

2. D. F. Wait, et al, “A Study of the Measurement of G/T using Cassiopeia A,” NBS AD-785 433, June 1974.

3. “IRE Standards on Electron Tubes: Definitions of Terms, 1962 (62 IRE 7.S2,” Proc IEEE, pp 434-442, March 1963.

4. C. T. Stelzried, “The Deep Space Network: Noise Temperature Concepts, Measurements, and Performance,” JF’L Publication 82-33, Jet Propulsion Laboratory, Pasadena CA Sept 15, 1982.

5. S. Silver, “Microwave Antenna Theory and Design”, McGraw Hill, 1949.

6. K. Bartos, et al, “Antenna Gain Calibration Procedure, ” JPL Internal Document D-3794, November 15, 1986.

7. W. M. Baars, et al, “The Absolute Spectrum of Cas A; An Accurate Flux Density Scale and a Set of Secondary Calibrators,”. Astron and Astrophys, **106**, 1977.

8. J. A. Turegano and M. J. Klein, “Calibration Radio Sources for Radio Astronomy: Precision Flux Density Measurements at **8420** MHz,” Astron and Astrophysics, 86, 1980.

9. M. J. Klein and C. T. Stelzried, “Calibration Radio Sources for Radio Astronomy: Precision Flux-density Measurements at 2295 MHz,” The Astronomical Journal, December 1976.

10. M. J. Klein and A. Freiley, "DSN Radio Source List for Antenna Calibration, ” JPL Internal Document D-3801 Rev B, September 25, 1987.

11. P.D. Batelaan, R, M. Goldstein, and C. T. Stelzried, “A Noise Adding Radiometer for Use in the DSN," JPL Publication 82-33, Jet Propulsion Laboratory, Pasadena CA, pp 66-69, Sept 30, 1970.

12. C. T. Stelzried, et al, “[1 SS-13 26-m Antenna Upgraded Radiometer System, ” JPL TDA PR 42-109, May 1992.

13. C.T. Stelzried, “Microwave Radiometer Calibrations,” JPL Document D-10496, January 29, 1993.

14. L. J. Skjerve, “Preliminary Documentation for DSS 13 Radiometer Program,” JPL Internal Document D-9292, January 1990.

15. C. T. Stelzried, "Operating Noise-Temperature Calibrations of Low-Noise Receiving Systems," Microwave Journal, 14, No. 6, p41, June 1971.

16. C. T. Stelzried, "Noise Adding Radiometer Performance Analysis," l-DA Progress Report 42-59, pp 98-106, Ott 1980.

17. C. T. Stelzried, "Non-linearity in Measurement Systems: Evaluation Method and Application to Microwave Radiometers," JPL TDA PR 42-91, Nov 1987.

18. P. G. Steffes, M. J. Klein and J. M. Jenkins, "Observations of the Microwave Emission of Venus from 1.3 to 3.6 cm," Icarus, 84, 83-92, 1992.

19. M. J. Klein and S. Gulkis, "Jupiter's Atmosphere: Observations and Interpretation of the Microwave Spectrum Near 1.25-cm Wavelength," Icarus, 35, 44-60, 1978.

20.1. dePater and S. T. Massie, "Models of the Millimeter-centimeter Spectra of the Giant Planets", Icarus, 62, 143-171, 1985

21. F. T. Ulaby, et al, Microwave Remote Sensing Active and Passive , **Vol 1** Addison-Wesley Press," 1981

22. M. Britcliffe, et al, "DSS-13 Beam Waveguide Antenna Project, " Phase I Final Report, JPL Internal Document D-8451, May 15, 1991.

23. M. S. Gatti, M. J. Klein and **'T.** B.H. Kuiper, **"32** GHz **Performance of the** DSS-14 70-Meter Antenna: 1989 Configuration," JPL TDA PR 42-99, Nov, 1989.

24. R. C. Clauss, et al, "Ruby Masers for Maximum G/TOP, " this issue.

Printed (1 1/19/93)

FIGURES

1. Microwave total power radiometer (TPR) block diagram

2. Schematic input system noise temperatures and output readings for a total power radiometer. The results of a linear and nonlinear analysis example are shown.

3. Experimental results from a total power radiometer linear and non-linear analysis as a function of uncalibrated radiometer output readings taken 11/10/92 on the D!3S-13 34-m antenna Ka-band non-optimized receiving system configuration.

4. Comparison of results from a linear and nonlinear analysis applied to the zenith noise temperature calibrations using the NAR and TPR on the DSS 1326-m antenna at 2,3 GHz (8/28/87).

5. Calibration of the time dependence of receiving system gain of the HEMT LNA/receiver operating at 33.68 GHz on the DSS 13 34-m BWG antenna. Calibrations were made with the OBSCAL program on 4/1/93 (DOY 091).

6. The measured dependence of the effective aperture efficiency, η, on radio source elevation for the DSS-13 34-m antenna operating at K_a-band (33.68 GHz); attenuation from the clear atmosphere has been removed.

7. Relationship between calculated error in G/T_{op} and the orbital period of Venus for measurements of the planet using a radiometer receiving system with a hypothetical 119'o non-lineaity.

Al
Figure Al. DSS-13 34-m antenna radio source difference calibration measurement errors using an unoptimized radiometer receiving system with about 11 % non-linearity and assuming various off source system noise temperatures.

APPENDIX A

RADIOMETER EQUATIONS AND APPLICATION TO RECEIVING SYSTEM NON-LINEARITY CORRECTION AND ERROR ANALYSIS

1. RADIOMETER EQUATIONS

The equations for calibrating radiometer receiving system gain and accounting for non-linearity are developed in the following. The results are applicable to not only the TPR but to NAR, Dicke and other radiometer configurations.

Consider the TPR shown in figure Al. The calibration method consists of recording the receiving system output readings designated R1, R2, R3, R4 and R5: output device input terminated, receiver input switched to the ant, ant+ calibration noise diode (ND), ambient load, and ambient load + ND, respectively. The readout device offset, R1 is subtracted from the original R2, R3, R4 and R5 readings. The offset corrected readings R2, R3, R4 and R5 correspond to system noise temperatures T2, T3, T4 and T5 in the following analyses. A linear analysis assumes equations of the form

$$T = B\,R \qquad \text{(Al)}$$

where

- T = system noise temperature with radiometer receiver input connected to the designated source, K
- $T4$ = $273.16 + T_p + T_e - T_c$, K
- T_p = ambient load temperature, C
- T_c = $0.024\,F,GHz$ (high frequency noise temperature correction, Ref Al), K
- T_e = receiving system noise temperature = $T_{lna} + T_f$, K
- T_{lna} = LNA noise temperature, K
- T_f = follow on amplifier noise temperature contribution
- R = radiometer receiver output device readings with receiving system input connected to the designated source defined for T, watts (typ)
- B = receiving system gain = T4/R4, kelvins/watt (typ)

The system noise temperature T2 ($=T_{op}$) with the receiving system LNA input connected to the antenna is defined previously with equation (8).

T_f is measured periodically (Ref A2) and Tlna is assumed calibrated in the laboratory' or field environment (Ref A3). From readings R3, and R5, measurements of the system noise temperatures T3 and T5 are obtained,. The noise temperature of the ND is measured with the receiver input connected to the antenna and to the ambient load as TN2 = T3 - T2 and TN4 = T5 - T4.

The analysis to quantify and correct the receiving system non-linearity assumes a quadratic non-linear corrected solution for system noise temperature TC in terms of the linear solution T.

$$TC = BC\ T2 + CC\ T2^2 \quad \text{(A2)}$$

using the measured noise temperatures from the linear analysis

$$T2C = BC\ T2 + CC\ T2^2 \quad \text{(A3)}$$

$$T3C = BC\ T3 + CC\ T3^2 \quad \text{(A4)}$$

$$T4 = BC\ T4 + CC\ T4^2 \quad \text{(A5)}$$

$$T5C = BC\ T5 + CC\ T5^2 \quad \text{(A6)}$$

TC4 has been replaced with T4 since this is a condition for setting the radiometer receiving system gain. Forcing equality for the corrected noise diode temperature TNC on the antenna and ambient load

$$TNC = T3C - T2C \quad \text{(A7)}$$

$$TNC = T5C - T4 \quad \text{(A8)}$$

The constants BC and CC are given by

$$CC = \frac{T5 - T4 - T3 + T2}{T4\,(T5 - T4 - T3 + T2) - (T5^2 - T4^2 - T3^2 + T2^2)} \quad \text{(A9)}$$

$$BC = 1 - CC\ T4 \quad \text{(A10)}$$

For a highly linear radiometer receiving system, CC approaches O and BC approaches 1. A radiometer receiving system linearity factor is defined by

$$FL = TC/T2C \quad \text{(A11)}$$

2. RADIOMETER PROGRAMS AND APPLICATION

These equations have been programmed in computer spreadsheet applications as RADPRE for radiometer pre-calibrations and RADOBS for observing calibrations. The input data format is the same for each program. The data can be formatted in CSV (comma separated value) files. Typically 6 sets of data are recorded for RADPRE in less than 10 minutes. The observing calibrations, analyzed with program RADOBS usually involve calibrations over many hours, appropriate for the users observing activities. Calibrating and monitoring the radiometer receiving system gain and linearity changes are important for the observing measurements accuracy and consistency. Typically the system hardware is maintained for suitable linearity and only the radiometer receiving system gain changes are used for correcting the observational data.

3. THE ERROR IN RADIO SOURCE DIFFERENCE MEASUREMENTS

These following equations can be used to estimate the error due to receiving system non-linearity in radio source antenna pointing "on-off" measurements, Assuming the linear analysis is in error and the non-linear is not (an approximation), the % error for a radio source difference measurement is given by

$$\% \text{ error} = 100\ ((T_S/T_SC) - 1\ ) \qquad \text{(Al 2)}$$

where

T_S = (Ton - l-off), K
T_SC = ($T_{on}C$ - $T_{off}C$, K
Ton = system noise temperature, on source, K
T_{off} = system noise temperature, off source (same sky region), K
Tone = system noise temperature, corrected, on source, K
$T_{off}C$ = system noise temperature, corrected, off source, K

using equation A3 and

$$T_{on}C = BC\ T_{on} + CC\ T_{on}^2 \qquad \text{(Al 3)}$$

with equations Al O and Al 2 and Ton= T_S +- T_{off},

$$\% \text{ error} = \frac{100\ CC\ (T4 - T_S - 2\ T_{off})}{CC\ (T4 - T_S - 2\ T_{off}) - 1} \qquad \text{(Al 4)}$$

Equation Al 4 is a maximum at T_S = O and goes **to zero if CC = O or**

$$T_S = T4 - 2\ T_{off} \qquad \textbf{(Al 5)}$$

The % error (equation Al 4) is shown in Figure A1 using the radiometer constants for the DSS 13 34-m antenna K_a-band TPR prior to optimizing the radiometer receiving system linearity (measured 11/1 0/92, CC = 3.33394 x 10^{-4} and T4 = 340.08 K) for T_{off} = 30, 50 and 70 K. These T_{off} temperatures approximate the Ka-band zenith system noise temperatures for future maser, present maser and present HEMT LNA operation, respectively. This plot shows that the non-linearity is maximum for low system and source noise temperatures and minimum for equation A15 satisfied. The radio source measurement errors are discussed further in the text.

Appendix A References

Al. C, T. Stelzried, "Correction of High Frequency Noise Temperature Inaccuracies," JPL TDA PR 42-111, November 15, 1992.
A2. C. T. Stelzried, "Improved RF Calibration Techniques:Daily System Noise Temperature Measurements," JPL Space Program Summary 37-42, Vol III, November 30, 1988.
A3. C. T. Stelzried, "The Deep Space Network Noise Temperature Concepts, Measurements and Performance," JPL Publication 82-33, September 15, 1982.

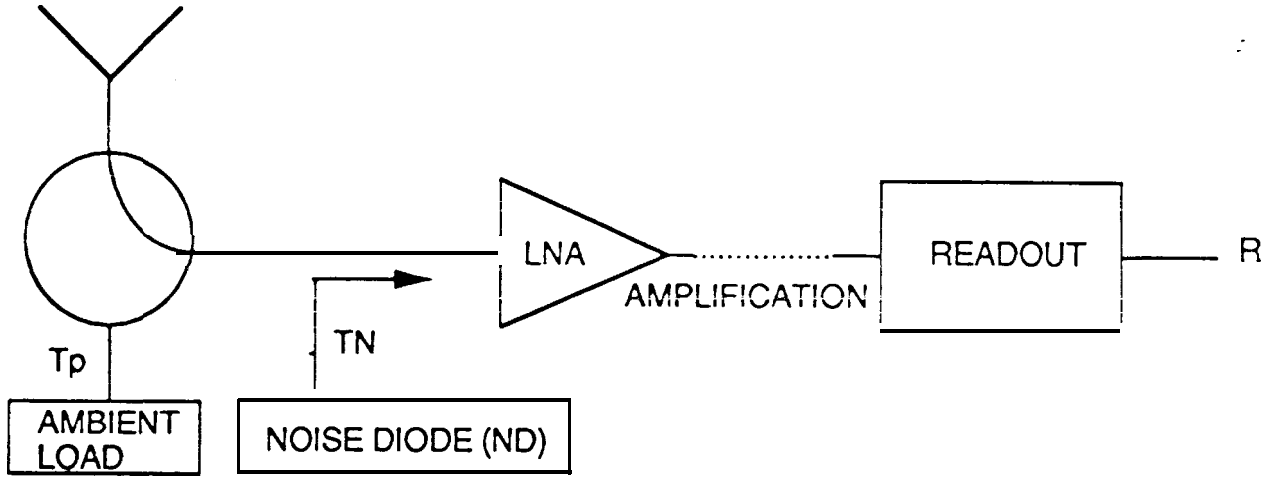

Figure 1 Microwave total power radiometer (TPR) block diagram

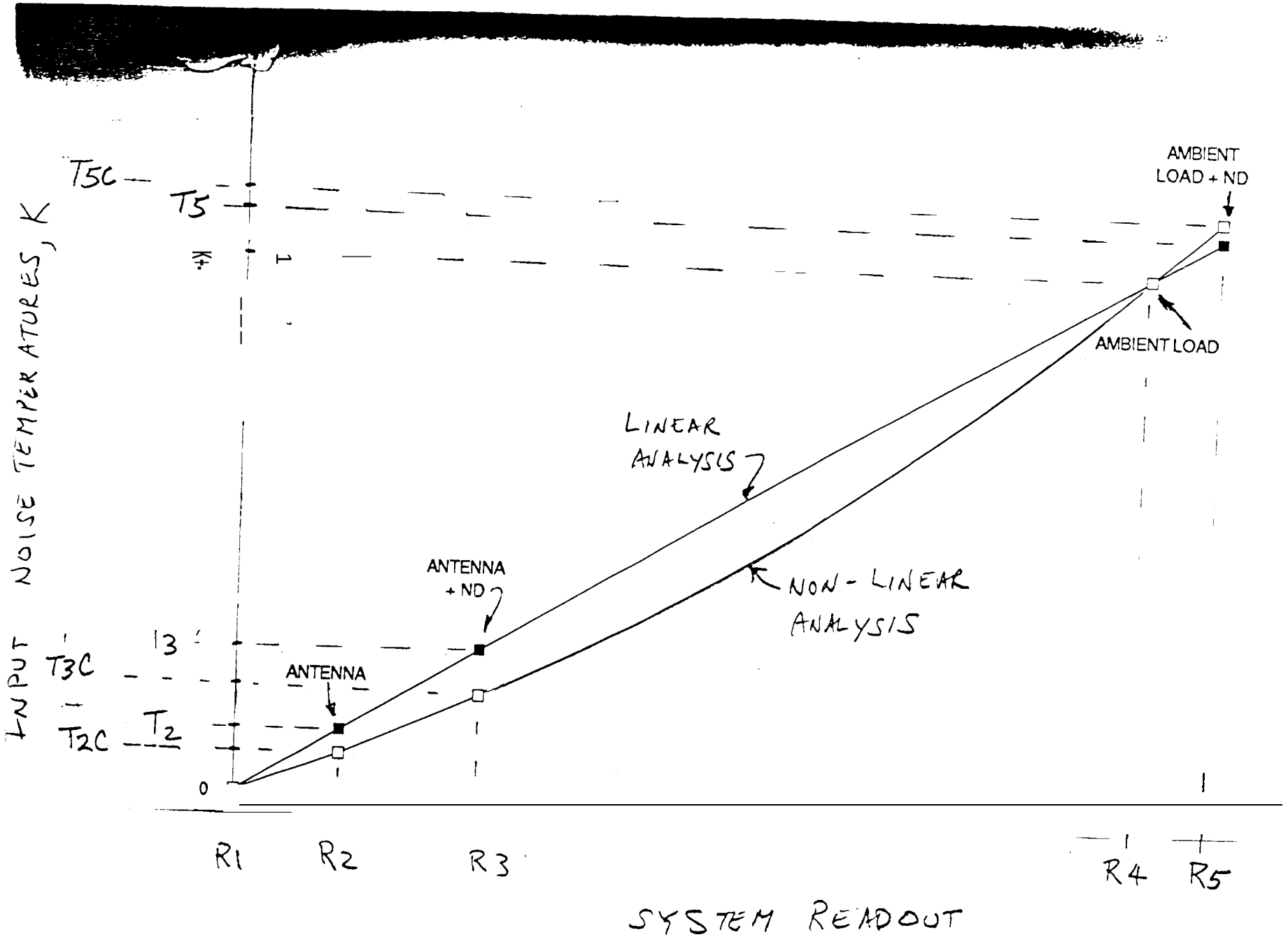

Figure 2. Schematic input system noise temperatures and output readings for a total power radiometer. The results of a linear and nonlinear analysis example are shown.

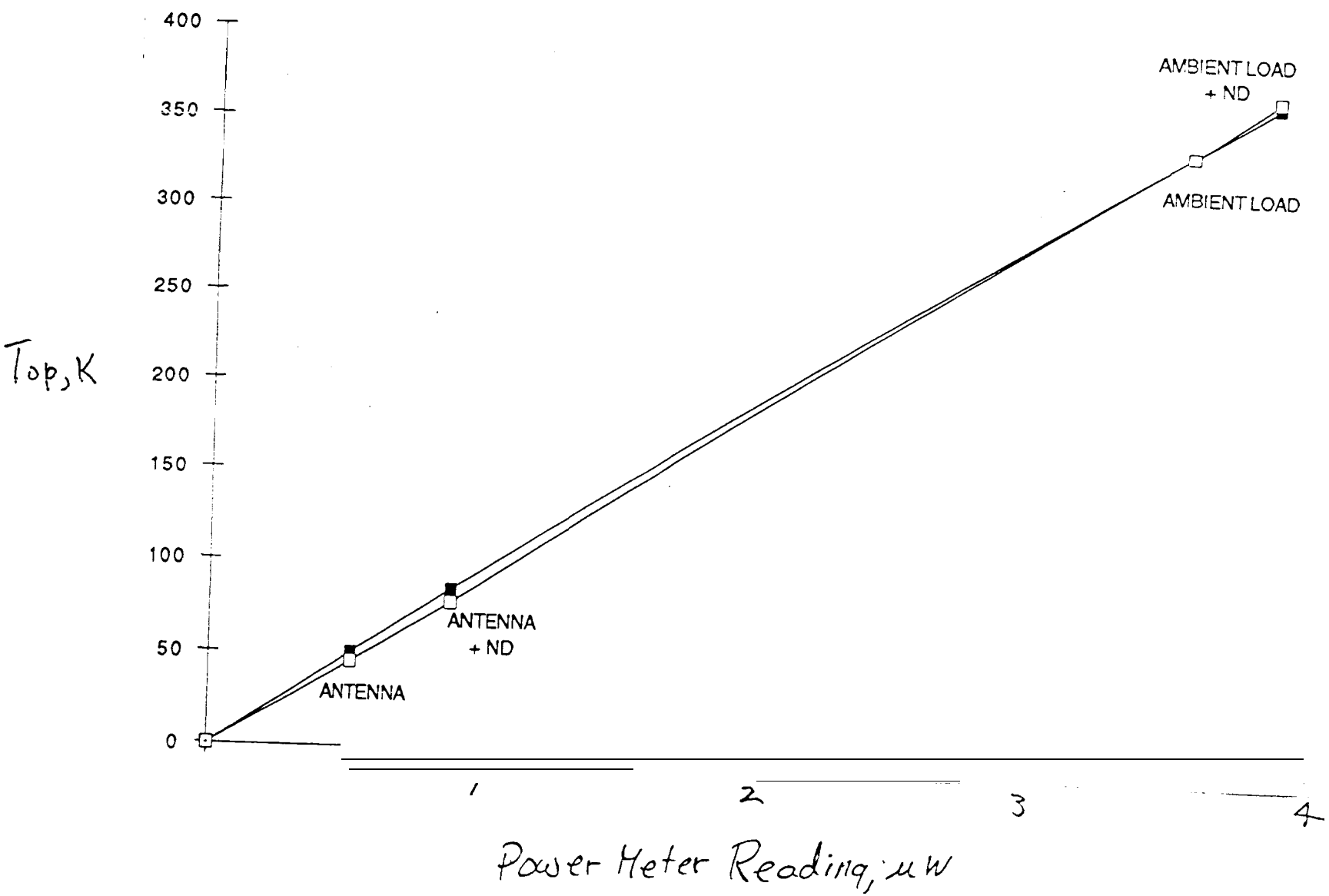

Figure 3. Experimental results from a total power radiometer linear and non-linear analysis as a function of uncalibrated radiometer output readings taken 11/ on the DSS-13 34-m antenna K_a-band non-optimized receiving system configuration.

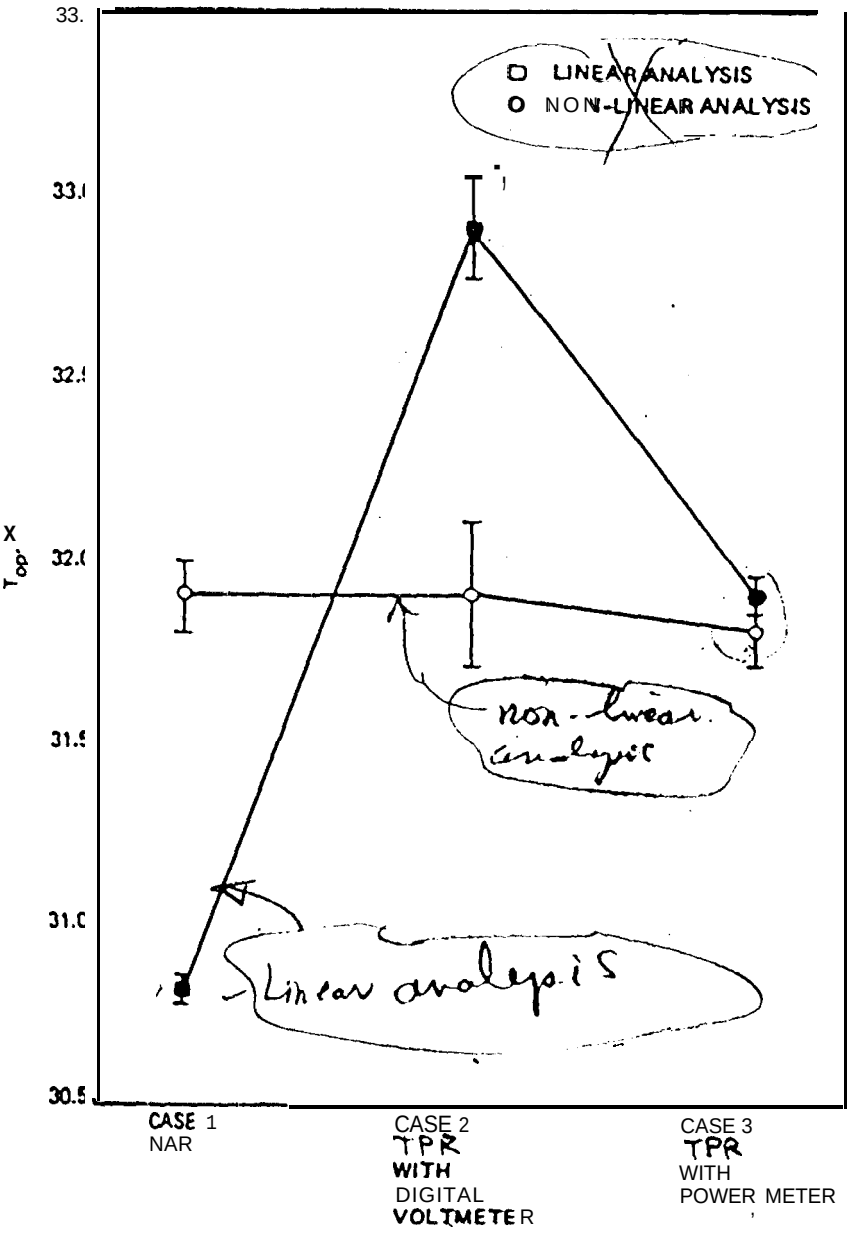

Figure 4. Comparison of results from a linear and nonlinear analysis applied to the zenith noise temperature calibrations using the NAR and TPR on the DSS 13 2&m antenna at 2.3 GHz (8/28/87).

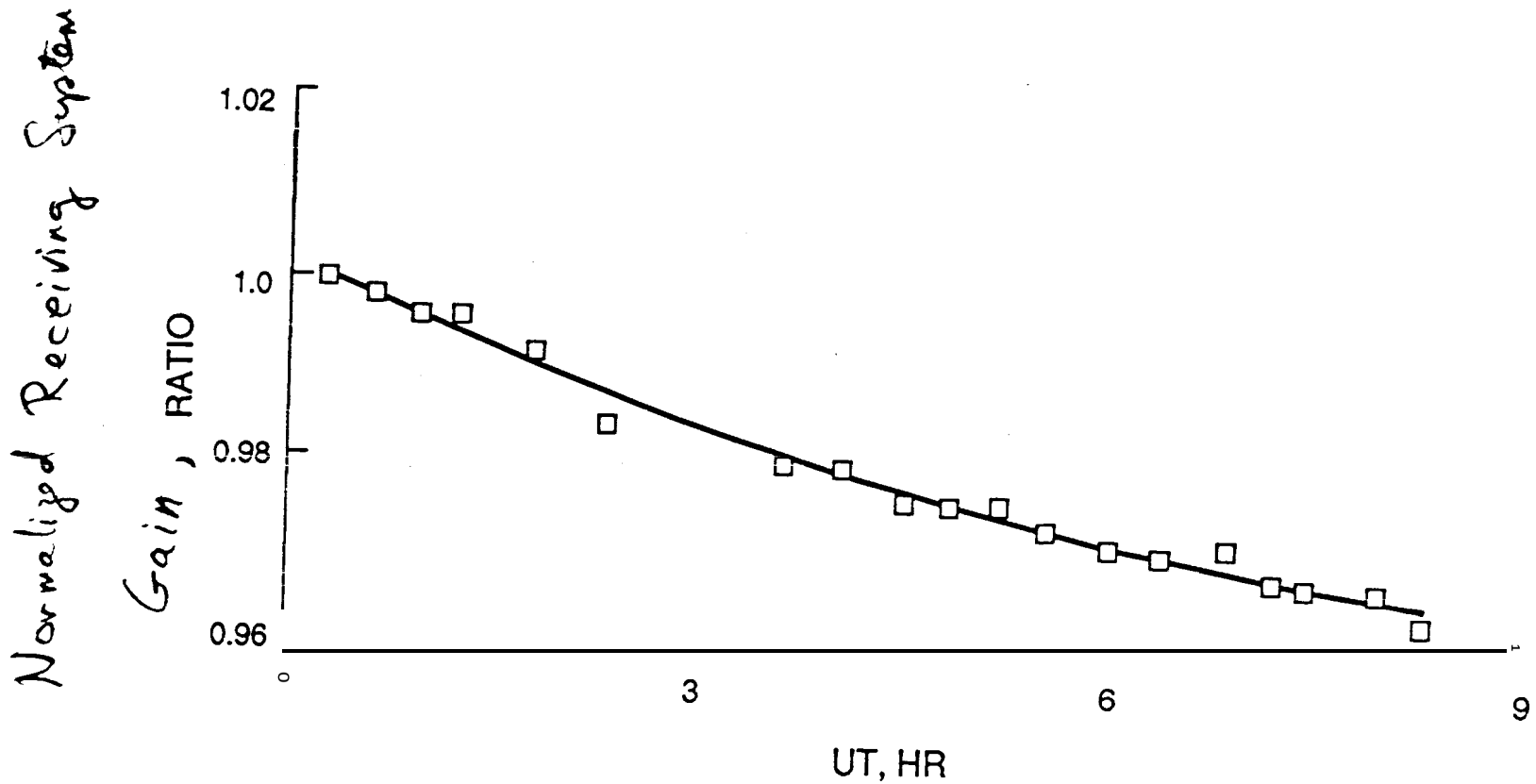

Figure 5. Calibration of the time dependence of receiving system gain of the HEMT LNA/receiver operating at 33.68 GHz on the DSS 13 34-m BWG antenna. Calibrations were made with the OBSCAL program on 4/1/93 (DOY 091).

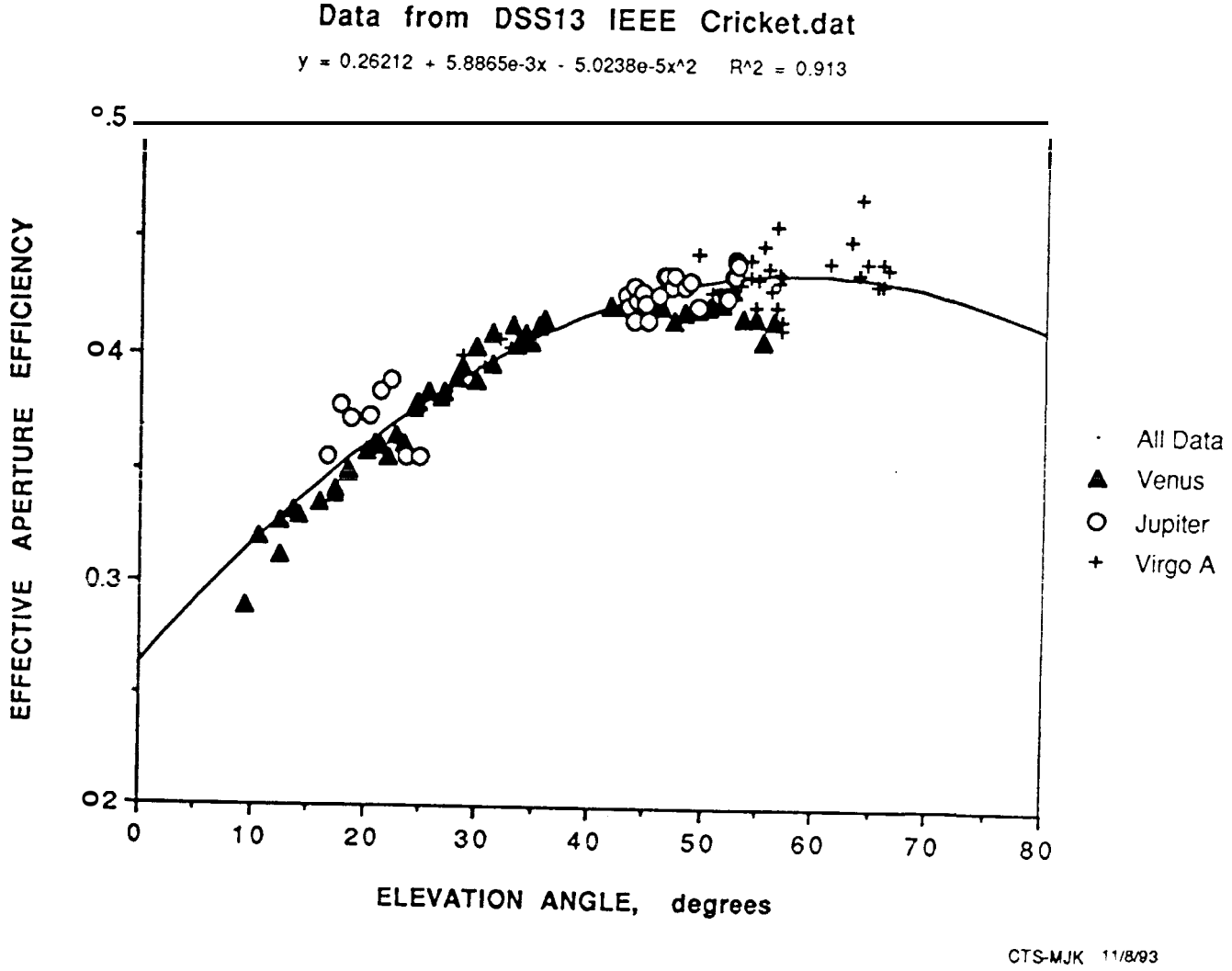

FIGURE

6. The measured dependence of the effective aperture efficiency, η , on radio source elevation for the DSS-13 34-m antenna operating at K_a-band (33.68 GHz); attenuation from the clear atmosphere has been removed.

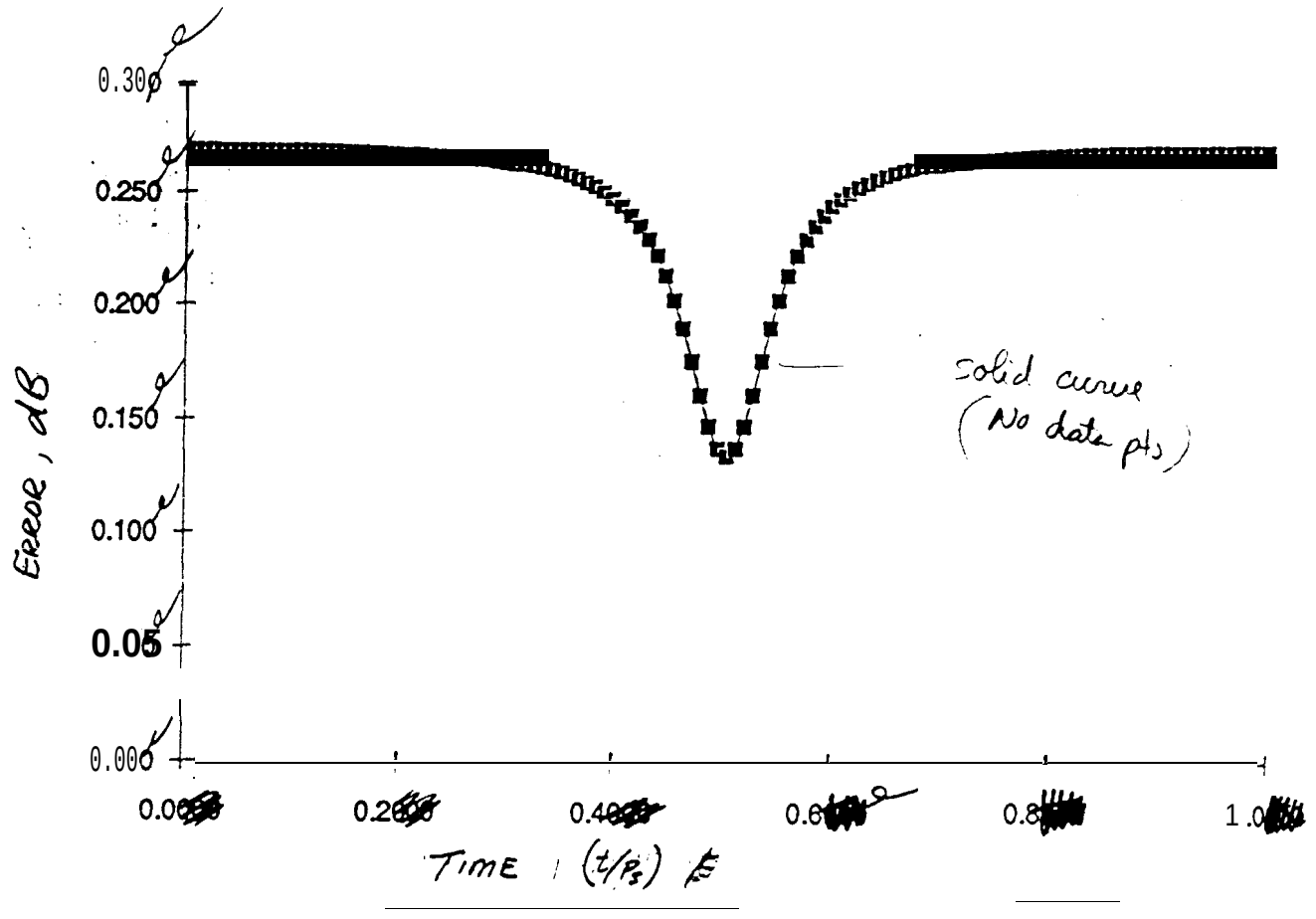

Figure 7. Relationship between calculated error **in G/TOP** and the orbital period of Venus for measurements of the planet using a radiometer receiving system with **a hypothetical** 11% non-lineaity.

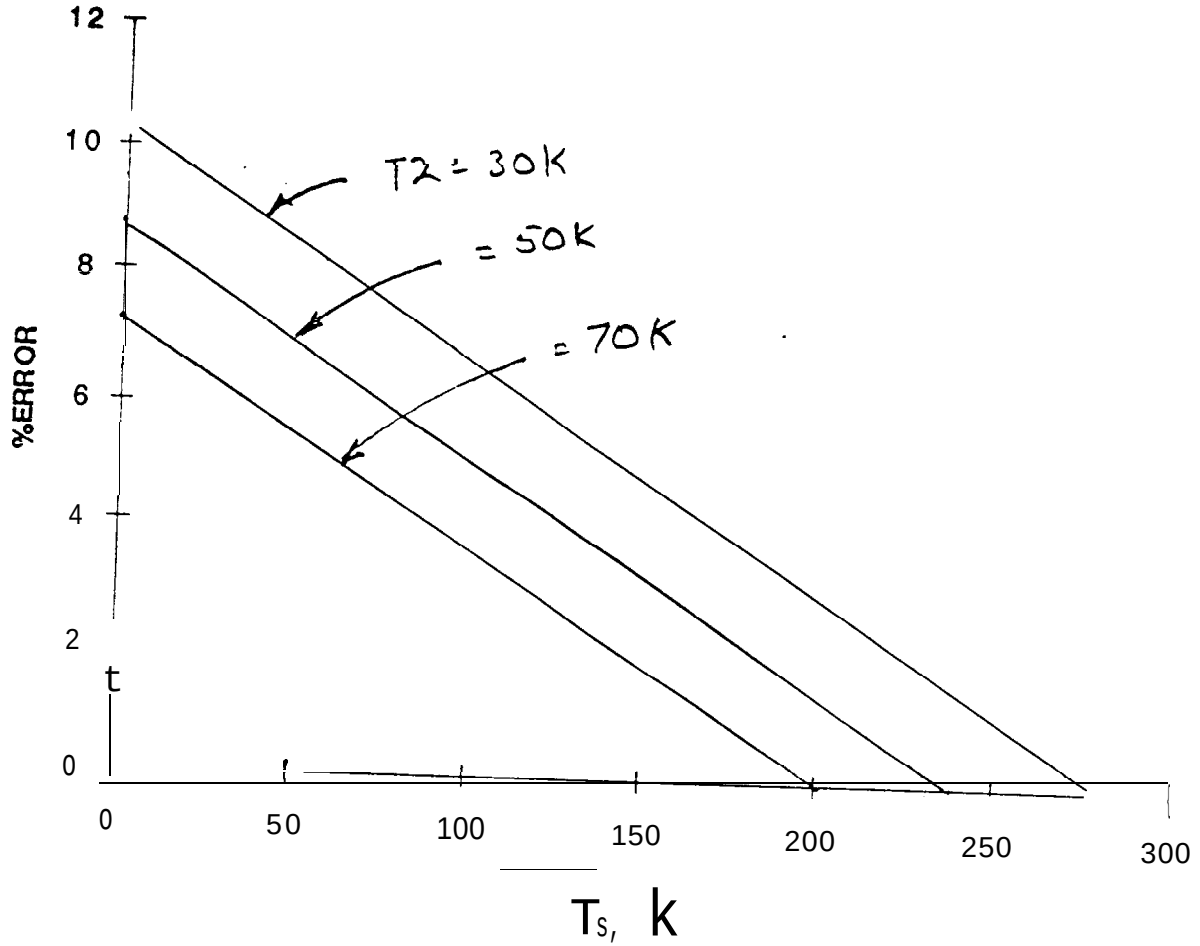

Figure A1

Figure Al. 0SS-13 34-m antenna radio source difference calibration measurement errors using an unoptimized radiometer receiving system with about 11 % non-linearity and assuming various off source system noise temperatures.